CrystEngComm

Accepted Manuscript

ROYAL SOCIETY OF CHEMISTRY

www.rsc.org/crystengcomm

Journal Name

RSCPublishing

ARTICLE

Cu^{2+} Under-Potential-Deposition Assisted Synthesis of Au and Au-Pd Alloy Nanocrystals with Systematic Shape Evolution

Cite this: DOI: 10.1039/x0xx00000x

Received 00th January 2012,
Accepted 00th January 2012

DOI: 10.1039/x0xx00000x

www.rsc.org/

Lei Zhang, Qiaoli Chen, Zhiyuan Jiang, Zhaoxiong Xie* and Lansun Zheng

The syntheses of noble metal nanocrystals (NCs) with systematic shape evolution have received extensive attentions in the research on nanomaterials. The introduction of foreign metal ions was one of the most effective ways to control the shape of the noble metals. However, most of the reports on the shape influence of the foreign metal ions focused on Ag^+. Herein, we systematically investigated the influence of Cu^{2+} on the structure evolution of Au NCs by forming under-potential-deposition atoms layer on the metal surface. The growth rate of atoms on high-index surfaces became more rapid than that on low-index facets, which caused the NCs evolved from trioctahedral to cubic and octahedral structures. In addition, by regulating the given amount of Cu, the Au-Pd alloy with different morphologies can also be prepared. Furthermore, we found that, the as-prepared HOH and cubic Au-Pd alloy NCs exhibited excellent performance in formic acid electro-oxidation in comparison with Pd black.

Introduction

Noble metal nanocrystals (NCs) have received extensive attention owing to their wide applications in numerous catalytic reactions.[1-7] Intensive studies have indicated that the catalytic performances of the noble metal NCs are largely determined by their shapes with different exposed surfaces.[8-13] Hence, the syntheses of noble metal NCs with systematic shape evolution is one of the most important topics in the research area of nanomaterials. According to our best knowledge, noble metal NCs with systematic shape evolution can be obtained by thermodynamic controlled synthesis and delicate control over the growth kinetics.[14-22] Specifically, thermodynamically controlled synthesis of noble metal NCs can be achieved by thermodynamically controlling surface energy of specific crystal faces via introducing specific surfactant, small molecules or foreign metal ions or adjusting supersaturation of crystal growth units in the growth medium during the crystal growth process. For the thermodynamically controlled synthesis, surfactant and small molecules-mediated syntheses of noble metal NCs with systematic shape evolution have been widely studied in recent years. However, there are few reports on the foreign metal ion-mediated preparation of shape-controlled NCs. Furthermore, almost all the reports about the shape influence of the foreign metal ions focused on Ag^+ ions. For example, Au nanocrystals with different morphologies, such as tetrahexahedra, nanocubes, nanorods and concave cubes, can be successfully synthesized with the introduction of trace amount of $AgNO_3$.[23-27] In these syntheses, the under-potential-deposition (UPD) of Ag on the Au surface stabilized the high index surfaces and caused the exposing of high index facets.

Recently, we found that UPD of Cu ions on Au-based alloy NCs surface also took place when introducing Cu species, which avoid the phase separation of Au and Pd via the galvanic displacement of Pd with UPD Cu on the surface.[28] As has been known, Cu UPD layer can be formed on different types of Au surfaces with different reduction potential.[29,30] Therefore, Cu^{2+} ions could be a promising foreign metal ion to regulate the growth kinetics of Au and Au-based alloy NCs, and finally affect their morphologies. Based on this point, we choose Cu^{2+} ion as the foreign ion to investigate its effect on the morphology evolution of Au and Au-based alloy NCs in this paper. It was found that the Au NCs from trioctahedra with {hhl} high index facets, to cubic and octahedral/plate-like structures could be synthesized by varying the concentration of Cu^{2+} ions in the growth solution. By analysing the X-ray photoelectron spectroscopy (XPS), we proposed that Cu UPD layer played a key role in the preparation of Au NCs with systematic shape evolution. The Cu atoms preferred to deposit on high-energy surfaces during the UPD process, leading to a faster growth rate of high energy surface and its disappearance in the final products. Such evolution law can also be applied in the syntheses of Au-Pd alloy NCs. Finally, we studied the

electrocatalytic properties of the as-prepared Au-Pd NCs with different morphologies.

Experimental

Materials

Chloroauric acid hydrated ($HAuCl_4 \cdot 4H_2O$, analytical grade), L-ascorbic acid (AA, analytical grade), Cetyltrimethyl trimethyl ammonium chloride (CTAC, 99%), copper(II) acetate ($Cu(CH_3COO)_2$, analytical grade) and hydrochloric acid (HCl, analytical grade) were purchased from Sinopharm Chemical Reagent Co. Ltd. (Shanghai, China). Palladium(II) chloride ($PdCl_2$, analytical grade) was purchased from Shanghai fine chemical materials institute. Pd black (metals basis, 99.9%) was purchased from Alfa Aesar. All reagents were used as received without further purification. All aqueous solutions were prepared with ultrapure water.

Preparation of 1 mmol/L H_2PdCl_4 solution

The H_2PdCl_4 solution (10 mmol/L) was prepared by dissolving $PdCl_2$ (0.1773 g) in a HCl (0.2 mol/L, 10 mL) solution and further diluting it to 100 mL with ultrapure water. A H_2PdCl_4 solution (1 mmol/L) was prepared by diluting a H_2PdCl_4 solution (10 mm) with ultrapure water.

Synthesis of Au NCs with systematic shape evolution

Firstly, a CTAC aqueous solution (3.0 mL, 40 mmol/L) was added into an aqueous $HAuCl_4$ solution (3.0 mL, 1.0 mmol/L). An aqueous $Cu(CH_3COO)_2$ solution (1.0 mmol/L) of 0.00mL, 0.30 mL or 1 mL was added into the solution to prepare Au NCs with {221}, {100} or {111} exposed surfaces, respectively. After homogeneous mixing, a freshly prepared aqueous AA solution (0.20 mL, 0.10 mol/L) was quickly added with a gentle shaking to this solution and left undisturbed for 20 min at 23 °C. After the reaction, the samples were centrifuged at 6000 rpm for 10 min and washed by ultrapure water for two times.

Synthesis of hexoctahedral (HOH) and cubic Au-Pd alloyed NCs

In a typical synthesis, an aqueous H_2PdCl_4 solution(1.0 mL, 1.0 mmol/L), a CTAC aqueous solution (3.0 mL, 0.04 mol/L) were added into an aqueous $HAuCl_4$ solution (3.0 mL, 1.0 mmol/L) in turn. An aqueous $Cu(CH_3COO)_2$ solution (1.0 mmol/L) of 0.30 mL or 1.00 mL was added into the solution to prepare HOH and cubic Au-Pd alloy NCs, respectively. After homogeneous mixing, a freshly prepared aqueous AA solution (0.20 mL, 0.10 mol/L) was quickly added with a gentle shaking to this solution and left undisturbed for about 12 hours at 23 °C. After the reaction, the samples were centrifuged at 6000 rpm for 10 min and washed by ultrapure water for two times.

Structural characterizations

The morphology and structure of the products were characterized by a scanning electron microscope (Hitachi, S-4800), a transmission electron microscope (JEOL, JEM-2100) and X-ray powder diffraction (XRD, Panalytical X-pert diffractometer with Cu-Kα radiation). The HAADF-STEM-EDS was performed on a FEI TECNAI F30 microscope operated at 300 kV. The surface compositions of the alloy were determined by a PHI QUANTUM2000 photoelectron spectrometer (XPS) using a monochromatic magnesium X-ray source. The binding energies were calibrated with respect to the signal for adventitious carbon (binding energy of 284.6 eV).

Electrochemical measurements

A glassy carbon electrode (diameter of 5 mm) was carefully polished and washed before every experiment. The ethanol suspensions of the as-prepared Pt NCs or Pt/C were dripped onto the surface of the glassy carbon electrode and dried at room temperature. CV measurements were carried out using an electrochemical workstation (CHI 631a, Shanghai Chenhua Co., China). Pt wire and a standard calomel electrode (SCE) were served as the counter and reference electrodes, respectively. All the electrode potentials in this paper are quoted versus the SCE. The glassy carbon electrode loaded with the as-prepared Au-Pd NCs or Pd black was electrochemical cleaned by continuous potential cycling between -0.20 and 0.90 V at 50 $mV \cdot s^{-1}$ in 0.5 mol/L H_2SO_4 until a stable cyclic voltammogram curve was obtained. The electrochemical reactivity and electrochemically active surface area of the catalysts were determined by the area of the oxygen desorption peaks in the cyclic voltammetry measurement performed in 0.5 mol/L H_2SO_4 electrolyte at a scan rate of 50 $mV \cdot s^{-1}$ (25 ºC).

Results and Discussion

Cu^{2+}-assisted synthesis of the Au NCs with systematic shape evolution

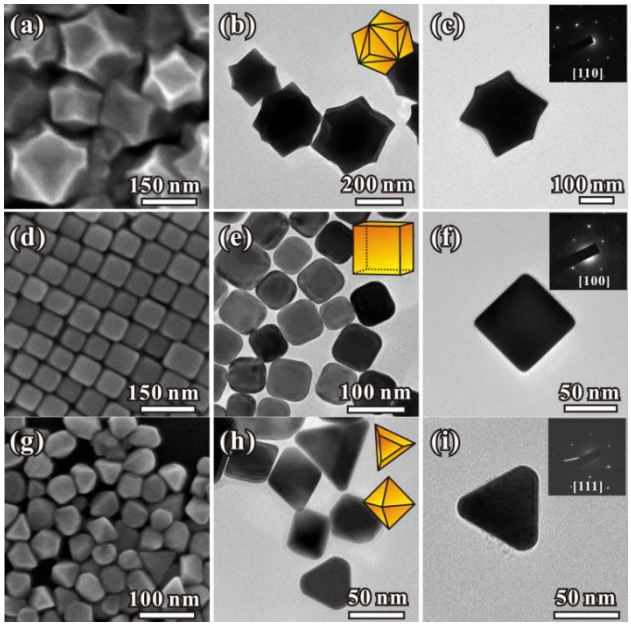

Fig. 1 The SEM and TEM images of (a-c) TOH Au NCs, (d-f) cubic Au NCs and (g-i) octahedral and plate-like Au NCs.

Fig. 1 shows the typical SEM and TEM images of the as-prepared three types of Au NCs. The Au NCs were prepared via a facile wet-chemical reduction route by using $HAuCl_4$ as metal sources, AA as reducing agent, CTAC as the capping agent and $Cu(CH_3COO)_2$ as the surface structure regulator. When no Cu^{2+} was not introduced in the system, the as-prepared Au performed a trioctahedral (TOH) shape with 24 {221} facets exposed (Fig. 1a and b). The outline of an individual nanocrystal coincide well with the TOH model when viewed from [110] direction (Fig. 1c). Several reports have showed that Au NCs with {hhl} facets can be obtained with similar experimental conditions.[31,32] When we introduced a small amount of $Cu(CH_3COO)_2$ at a Au/Cu molar ratio of 10:1, the morphology of as-prepared Au NCs evolved from TOH to cubic structure (Fig. 1d and e). In this case, the surface of an individual Au cube is smooth by observing from the [100] direction (Fig. 1f). When the amount of Cu^{2+} was increased to the Au/Cu molar ratio of 3:1, we obtained triangular plate and octahedron (Fig. 1g and h). It has been well characterized that the Au octahedrons are exposed by {111} surfaces. To investigate the surface structure of plate-like nanocrystals, TEM image and corresponding selected area electron diffraction (SAED) patterns were studied. Fig. 1i showed that the triangular plate-like NCs are also single crystals. Such a special plate can be thought to be evolved from an octahedron by cutting the model along {111} surface. Therefore, the plate-like NCs are also enclosed by {111} facets. According to previous published reports, the two types of polyhedrons are all exposed by {111} facets.[33-35] To further demonstrate the above mentioned morphology evolution tendency, we finely controlled the amount of $Cu(CH_3COO)_2$ and found that the Au NCs might evolve from trioctahedra to tetrahexahedra, then to cubes, cuboctahedra and ocatehedra with the increase of $Cu(CH_3COO)_2$ concentration, as shown in Fig. 2. These results also indicate that the Cu species played a pivotal role in controlling the morphology of the Au NCs.

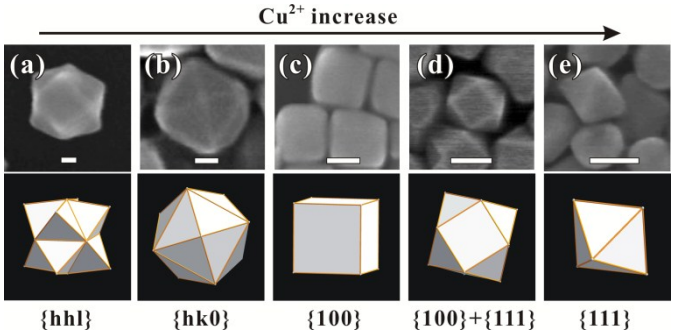

Fig. 2 A series of Au NCs obtained by finely controlled the amount of $Cu(CH_3COO)_2$. The Au/Cu molar ratio was tuned from (a) 1:0 to (b) 30:1, (b) 20:1, (c) 10:1, (d) 6:1 and (e) 3:1, respectively. (Scale bar: 50 nm)

To investigate whether the introduced Cu^{2+} was incorporated into the as-prepared Au NCs, we further characterized the composition of the obtained NCs by XRD, energy-dispersive X-ray (EDX) and XPS. The XRD partterns of these three types Au NCs with respectively exposed {221}, {100} or {111} facets, all match the fcc crystalline Au structure (JCPDS number: 04-0784) very well, which means that Cu do not exist in the as-prepared NCs (Fig. S1a). The EDX spectroscopy equipped on SEM also showed that no obvious Cu signal observed in the particles (Fig. S1, b-d). This evidence indicated that Cu has not been doped into the lattice of Au NCs. To further investigate how $Cu(CH_3COO)_2$ affected the shape evolution of the NCs, the surfaces of the NCs were detected by X-ray photoelectron spectroscopy (XPS). As shown in Fig. 3, two weak binding energy peaks at 931.9 eV and 953.2 eV were detected in the XPS spectra of Au NCs with {100} and {111} facets, which should be assigned to Cu $2p_{3/2}$ and Cu $2p_{1/2}$ of metallic Cu^0. This result indicated that a trace amount of Cu may exist on the surface of Au NCs. Inductively coupled plasma atomic emission spectroscopy (ICP-AES) also showed that the content of Cu in the NCs with {100} and {111} facets were 0.2% and 0.3%, respectively. As we know, Cu^{2+} can be reduced to Cu^0 on the surface of Au NCs at a more positive potential than that of $Cu^{2+/0}$ through the UPD path. We speculate the trace amount of Cu^0 on the surface of the NCs was caused by UPD-like deposition as Cu^{2+} ions can not be solely reduced in the current reaction condition.

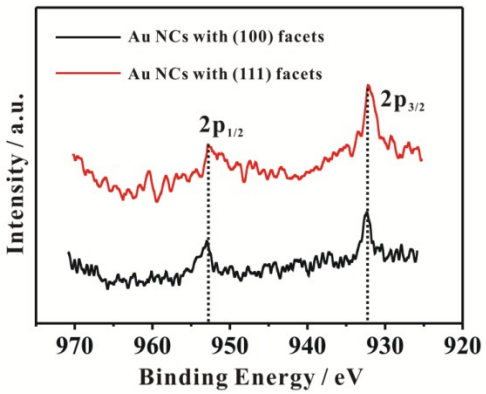

Fig. 3 The XPS spectrum of Au NCs with {100} and {111} facets showed the existence of Cu on the surface of the NCs.

Furthermore, Cu atoms preferred to deposit on the high-index surfaces during the UPD process, as high-index surfaces are much more active compared to relative low-index surfaces. Once Cu atoms have been deposited on the seeds via UPD like process, they can subsequently reduce $AuCl_4^-$ to elemental Au *via* a galvanic replacement. Meanwhile, Cu atoms are re-oxidized to Cu^{2+} ions. With the help of galvanic replacement of Cu UPD layer, the growth rate on high-index surfaces became rapid than that on low-index facets and this tendency increased with the increase of the concentration of Cu^{2+} ions, which caused the evolution of the surfaces of final product from high index facets to low-index facets. This systematic evolution law was different from that caused by Ag^+, where the UPD Ag atoms stabilized the high-index facets.[23-27] From the viewpoint of the standard reduction potential (SRP), the SRP of Cu^{2+} is

0.34V, while the SRP of Ag^+ is 0.8V. It can be seen that, the SRP of Ag was very close with that of Au, which means that the galvanic replacement is hard to carry on when an Ag UPD layer formed on Au seeds. Therefore, the Ag UPD layer may stabilize and reduce the growth rate of the high-index facets and causing the NCs exposed with relative high-energy facets.

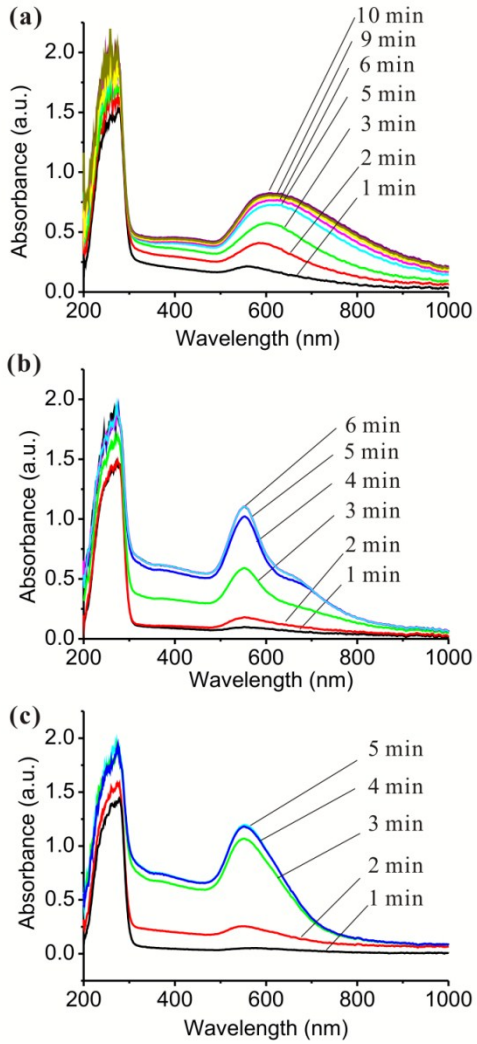

Fig. 4 In situ UV/Vis absorption spectra during the formation of (a) TOH, (b) cubic and (c) octahedral/plate-like Au NCs, respectively.

To get deep insight into the influence of Cu^{2+} ions on the shape evolution of Au NCs, in-situ UV/Vis absorption spectra were conducted to monitor the formation rate of the final products (Fig. 4). The UV/Vis absorption spectra were recorded every minute. As shown in Fig. 4, obvious absorption band at about 560–600 nm was observed during the growth of the Au NCs, which is ascribed to the surface plasmon resonance (SPR) of the as-prepared Au particles. Fig. 4a shows that the UV/Vis spectra for the reaction without Cu^{2+} did not change any more after 9 min, suggesting that the growth process had finished. When the amount of introduced of Cu^{2+} increased to 0.3 and 1 μmol, the reaction time reduced to 5 min and 4 min as shown in Fig. 4b and c, respectively. The result suggests that the reaction rate was accelerated with the introduction of Cu^{2+}. On the basis of the above results, it can be concluded that Cu UPD process accelerated the growth rate of Au NCs, especially the high-index facets, leading to the formation of Au NCs with systematic shape evolution from TOH to cubic and octahedral/plate-like structures.

Cu^{2+}-assisted synthesis of the Au-Pd alloy NCs with systematic shape evolution

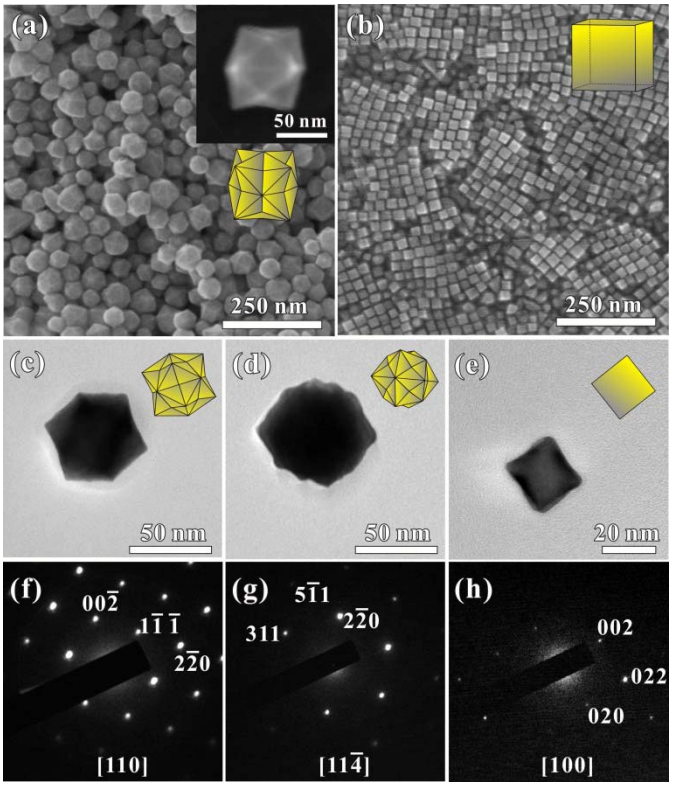

Fig. 5 (a, b) The SEM images of HOH and cubic Au-Pd alloy NCs obtained by introduction of different amount of $Cu(CH_3COO)_2$; (c, d, f and g) TEM images and SAED patterns of the HOH Au-Pd alloy NCs; (e, h) TEM image and SAED pattern of cubic Au-Pd alloy NCs.

The evolution of morphology which caused by Cu^{2+} can also be applied in the synthesis of Au-Pd alloy. In our previous work, we found that, the addition of Cu can avoid the separation of Au and Pd due to the UPD of Cu and following galvanic displacement.[28] Herein, we focus on the investigation of the influence on the morphology of the Au-Pd alloy NCs through Cu UPD process. When we only introduce 1.0 mL H_2PdCl_4 (1 mM) in the system of preparing TOH Au NCs (the molar ratio of Au and Pd is 3:1), the surface of the as-prepared NCs was rough (Fig. S2), indicating Au and Pd nucleated separately. With the introduction of 0.3 mL $Cu(CH_3COO)_2$ (1mM), the separation of Au and Pd can be avoided and very uniform NCs with smooth surface was prepared (Fig. 5a). The as-prepared NCs, with the average size of 50 nm, displayed a HOH shape with {hkl} facets. When viewing from the [110] and [$11\bar{4}$] directions, the individual one crystal matched HOH model well

(Fig. 5c, d, f and g). With the addition of 1.0 mL $Cu(CH3COO)_2$ (1mM), the products performed a cubic shape, instead of the HOH structure with {hkl} facets (Fig. 5b). The TEM image and SAED pattern suggest that the cubes are exposed by {100} facets (Fig. 5e and h). Elemental mapping analysis (Fig. S3) demonstrates that the distribution range of Au and Pd are completely overlapped, indicating the formation of Au-Pd alloy.

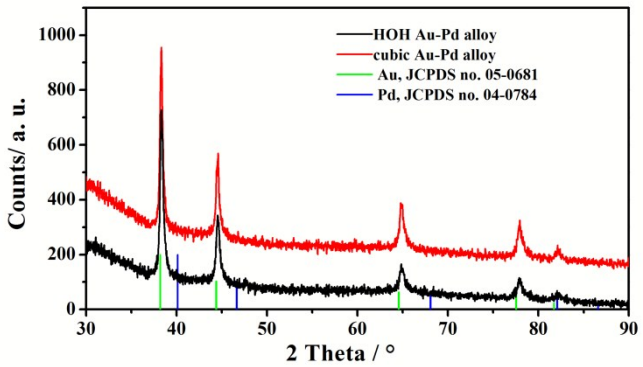

Fig. 6 XRD pattern of the HOH and cubic Au-Pd alloy NCs obtained by tuning the amount of introduced Cu species, indicating the formation of alloy structure.

The alloy structure can further be confirmed through the XRD pattern. The XRD pattern of the HOH and cubic Au-Pd alloy NCs showed that every diffraction peak appeared between the corresponding peak positions of pure fcc-structured Au and Pd (Fig. 6), suggesting the successful formation of Au-Pd alloy. According to Vegard's law,[36] which states that the crystal cell parameter of an alloy is linearly related to its composition, the Pd content in the HOH and cubic Au-Pd alloy can be determined to be 9.9% and 9.3%, respectively. To further determine the amount of each component in the HOH and cubic Au-Pd NCs, the samples were analysed by ICP-AES. The Pd content in the HOH and cubic Au-Pd alloy was measured to be 10.8% and 9.8%, respectively. The ICP-AES results agreed well with that measured by XRD pattern. In addition, the ICP-AES results show that 0.3% and 0.4% of Cu exist in the HOH and cubic alloy NCs, respectively, indicating trace amount of Cu deposited on the surface of the Au-Pd alloy NCs. On the basis of the above results, it can be concluded that Cu^{2+} played two important roles during the formation of HOH and cubic Au-Pd alloyNCs: 1) performing as the catalyst for the formation of Au-Pd alloy; 2) the influence on the morphology of the alloy NCs through UPD process.

Electrochemical properties of the as-prepared Au-Pd alloy NCs

In the above part of the article, we successfully synthesized HOH and cubic Au-Pd alloy NCs. To investigate the catalytic properties of the Au-Pd alloy, electrocatalytic oxidation of formic acid was used to characterize the catalytic activity of the as-prepared alloy NCs. Fig. 7a shows cyclic voltammogram (CV) curves in a mixture of 0.50 M H_2SO_4 + 0.25 M HCOOH solution, using the obtained HOH and cubic Au-Pd alloy NCs with 10% Pd as working electrodes, respectively. The current densities were normalized to the electrochemically active surface areas (ECSAs), which were determined by the area of the oxygen desorption peaks in the cyclic voltammetry measurement performed in 0.5 mol/L H_2SO_4 electrolyte at a scan rate of 50 $mV \cdot s^{-1}$ (25 ºC). As shown in Fig. 7a, the Au-Pd alloy with {hkl} facets exhibited the best catalytic activity because of the high-density atomic steps and kinks on high-index surfaces. To evaluate the electrocatalytic stability of the as-prepared Au-Pd alloy catalysts, chronoamperometric experiments were carried out (Fig. 7b). In this test, we found that the stabilities of these HOH and cubic Au-Pd alloy NCs catalysts were all much better than that of Pd black. The highest electrocatalytic ability of the HOH Au-Pd alloy NCs mainly originates from the synergism effect of the {hkl} high-energy facets and the Au-Pd alloy.

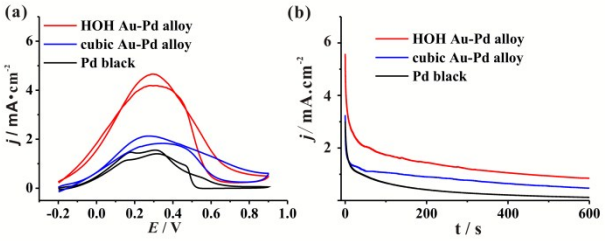

Fig. 7 (a) CV curves measured on the HOH and cubic Au-Pd alloy NCs and Pd black in an N_2-purged 0.50 M H_2SO_4 + 0.25 M HCOOH solution, respectively. Scan rate: 50 mV/s. (b) current–time curves of formic acid oxidation measured on the three kinds of nanocatalysts in 0.50 M H_2SO_4 + 0.25 M HCOOH solution at 0.30 V.

Conclusions

Au NCs with systematic shape evolution from TOH to cubic and octahedral/plate-like structures are obtained with the assistance of Cu^{2+}. We systematically investigated the composition of the as-prepared Au NCs by EDX, XPS and XRD and found that Cu^{2+} played as the surface structure regulator during the growth process. It can be concluded that the reaction rate, especially the growth rate of high-index surfaces, has been greatly promoted by the Cu UPD process and the subsequent galvanic replacement reaction. As the growth rate of atoms on high-index surfaces became more rapid than that on low-index facets, the obtained NCs evolved from trioctahedral to cubic and octahedral structures. The influence of morphology which caused by Cu^{2+} can also be applied in the synthesis of Au-Pd alloy. HOH and cubic Au-Pd alloy NCs with 10% content of Pd have been successfully synthesized. The as-prepared Au-Pd alloy NCs all performed better activity and stability for the electrocatalitic oxidation of formic acid than commercial Pd black.

Acknowledgements

This work was supported by the National Natural Science Foundation of China (Grant Nos. 21171142, 21171141, 21131005, and 21333008), the National Basic Research Program of China (Grant Nos. 2011CBA00508 and 2015CB932301).

Notes and references

State Key Laboratory of Physical Chemistry of Solid Surfaces, Collaborative Innovation Center of Chemistry for Energy Materials, and Department of Chemistry, College of Chemistry and Chemical Engineering, Xiamen University, Xiamen 361005, China
zxxie@xmu.edu.cn

Electronic Supplementary Information (ESI) available: [XRD and EDS spectrum of the TOH, cubic and octahedral/plate-like Au NCs; SEM images, TEM images and EDS spectrum of the Au NCs obtained in the presence of $AgNO_3$; SEM and TEM images of Au-Pd bimetallic NCs obtained in the absence of $Cu(CH_3COO)_2$; Cross-sectional compositional line-scanning profile of the HOH and cubic Au-Pd alloy. This material is available free of charge via the Internet at http://pubs.acs.org]. See DOI: 10.1039/b000000x/

References

1. A. S. Aricò, P. Bruce, B. Scrosati, J. M. Tarascon and W. V. Schalkwijk, *Nat. Mater.* 2005, **4**, 366.
2. G. A. Somorjai and C. J. Kliewer, *React. Kinet. Catal. Lett.*, 2009, **96**, 191.
3. Z. M. Peng and H. Yang, *Nano Today*, 2009, **4**, 143-164.
4. E. Antolini, *Energy Environ. Sci.*, 2009, **2**, 915.
5. H. Zhang, M. Jin and Xia, Y. *Angew. Chem. Int. Ed.*, 2012, **51**, 7656.
6. M. R. Langille, J. Zhang and C. A Mirkin, *Angew. Chem. Int. Ed.*, 2011, **50**, 3543.
7. D. Wang and Y. Li, *Adv. Mater.*, 2011, **23**, 1044.
8. Z. Jiang, Q. Kuang, Z. Xie and L. Zheng, *Adv. Funct. Mater.*, 2010, **20**, 3634.
9. Q. Kuang, X. Wang, Z. Jiang, Z. Xie and L. Zheng, *Acc. Chem. Res.*, 2014, **47**, 308.
10. A. R. Tao, S. Habas and P. D. Yang, *Small*, 2008, **4**, 310.
11. R. Narayanan and M. A. El-Sayed, *Nano Lett.*, 2004, **4**, 1343.
12. W. X. Niu and G. B. Xu, *Nano Today*, 2011, **6**, 265.
13. Z. Quan, Y. Wang, and J. Fang, *Acc. Chem. Res.*, 2013, **46**, 191.
14. J. Zhang, C. Hou, H. Huang, L. Zhang, Z. Jiang, G. Chen, Y. Jia, Q. Kuang, Z. Xie and L. Zheng, *Small*, 2013, **9**, 538.
15. H. Lin, Z. Lei, Z. Jiang, C. Hou, D. Liu, M. Xu, Z. Tian and Z. Xie, *J. Am. Chem. Soc.*, 2013, **135**, 9311.
16. H. L. Wu, C. H. Kuo and M. H. Huang, *Langmuir*, 2010, **26**, 12307.
17. J. Zhang, L. Zhang, Y. Jia, G. Chen, X. Wang, Q. Kuang, Z. Xie and L. S. Zheng, *Nano Res.*, 2012, **5**,181.
18. T. K. Sau and C. J. Murphy, *J. Am. Chem. Soc.*, 2004, **126**, 8648.
19. J. W. Hong, S. U. Lee, Y. W. Lee and S. W. Han, *J. Am. Chem. Soc.*, 2012, **134** , 4565.
20. L. Zhang, D. Q. Chen, Z. Y. Jiang, J. W. Zhang, S. F. Xie, Q. Kuang, Z. X. Xie and L. S. Zheng, *Nano Res.*, 2012, **5**,181.
21. S. Rej, K. Chanda, C. Y. Chiu and M. H. Huang , *Chem. Eur. J.*, 2014, **20**, 15991.
22. M. H. Huang and C. Y. Chiu, *J. Mater. Chem. A*, 2013, **1**, 8081.
23. T. Ming, W. Feng, Q. Tang , F. Wang, L. D. Sun, J. F. Wang and C. H. Yan, *J. Am. Chem. Soc.*, 2009, **131**, 16350.
24. J. Zhang, R. M. Langille, L. M. Personick, K. Zhang, S. Y. Li and A. C. Mirkin, *J. Am. Chem. Soc.*, 2010, **132**, 14012.
25. F. Kim, J. H. Song, and P. D. Yang, *J. Am. Chem. Soc.*, 2002, **124**, 14317.
26. D. Seo, J. C. Park and H. Song, *J. Am. Chem. Soc.*, 2006, **128**, 14863.
27. L. M. Personick, R. M. Langille, J. Zhang and A. C. Mirkin, *Nano Lett.*, 2011, **11**, 3394.
28. L. Zhang, J. Zhang, Q. Kuang, S. Xie, Z. Jiang, Z. Xie and L. Zheng, *J. Am. Chem. Soc*., 2011, **133**, 17114.
29. A. Kuzumea, E. Herrerob, J. M Feliub, R. J. Nicholsa and D. J. Schiffrin, *J Electroanal. Chem.*, 2004, **570**, 157.
30. S. Manne, P. K. Hansma, J. Massie, V. B. Elings and A. A. Gewirth, *Science*, 1991 , **251** , 183.
31. Y. Ma, Q Kuang, Z. Jiang, Z. Xie, R. Huang and L. Zheng, *Angew. Chem. Int. Ed.*, 2008, **47**, 8901.
32. Y. Yu, Q. B. Zhang, X. M. Lu and J. Y. Lee, *J. Phys. Chem. C*, 2010, **114**, 11119.
33. Y. Xia, Y. J. Xiong, B. Lim and S. E. Skrabalak, *Angew. Chem. Int. Ed.*, 2009, **48**, 60.
34. Z. L. Wang, *J. Phys. Chem. B*, 2000, **104**, 1153.
35. Y. Xiong, J. M. McLellan, J. Chen, Y. Yin, Z. Y. Li and Y. Xia, *J. Am. Chem. Soc.*, 2005, **27**, 17118.
36. A. R. Denton and N. W. Ashcroft, *Phys. Rev. A*, 1991, **43**, 3161.

